

*Stability analysis of a steady state of a model describing Alzheimer's disease and interactions with prion proteins*

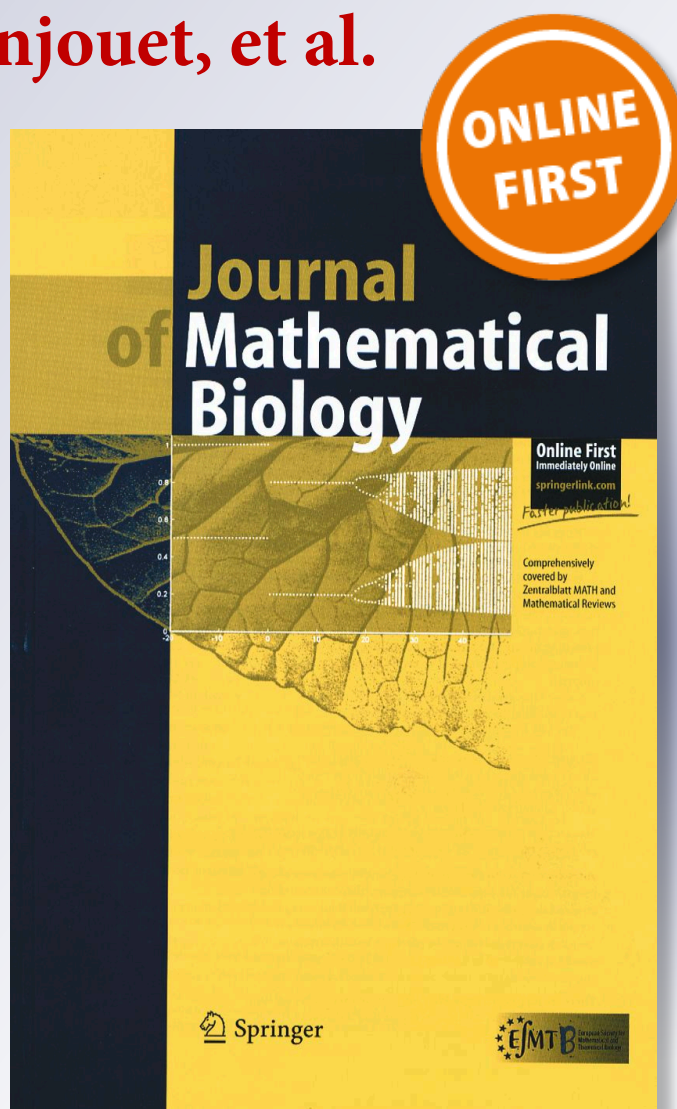
**Mohammed Helal, Angélique Igel-Egalon, Abdelkader Lakmeche, Pauline Mazzocco, Angélique Perrillat-Mercerot, Laurent Pujo-Menjouet, et al.**

**Journal of Mathematical Biology**

ISSN 0303-6812

J. Math. Biol.

DOI 10.1007/s00285-018-1267-1



**Your article is protected by copyright and all rights are held exclusively by Springer-Verlag GmbH Germany, part of Springer Nature. This e-offprint is for personal use only and shall not be self-archived in electronic repositories. If you wish to self-archive your article, please use the accepted manuscript version for posting on your own website. You may further deposit the accepted manuscript version in any repository, provided it is only made publicly available 12 months after official publication or later and provided acknowledgement is given to the original source of publication and a link is inserted to the published article on Springer's website. The link must be accompanied by the following text: "The final publication is available at [link.springer.com](http://link.springer.com)".**



## Stability analysis of a steady state of a model describing Alzheimer's disease and interactions with prion proteins

Mohammed Helal, et al. [full author details at the end of the article]

Received: 17 October 2017 / Revised: 9 April 2018  
© Springer-Verlag GmbH Germany, part of Springer Nature 2018

### Abstract

Alzheimer's disease (AD) is a neuro-degenerative disease affecting more than 46 million people worldwide in 2015. AD is in part caused by the accumulation of  $A\beta$  peptides inside the brain. These can aggregate to form insoluble oligomers or fibrils. Oligomers have the capacity to interact with neurons *via* membrane receptors such as prion proteins ( $\text{PrP}^{\text{C}}$ ). This interaction leads  $\text{PrP}^{\text{C}}$  to be misfolded in oligomeric prion proteins ( $\text{PrP}^{\text{ol}}$ ), transmitting a death signal to neurons. In the present work, we aim to describe the dynamics of  $A\beta$  assemblies and the accumulation of toxic oligomeric species in the brain, by bringing together the fibrillation pathway of  $A\beta$  peptides in one hand, and in the other hand  $A\beta$  oligomerization process and their interaction with cellular prions, which has been reported to be involved in a cell-death signal transduction. The model is based on Becker–Döring equations for the polymerization process, with delayed differential equations accounting for structural rearrangement of the different reactants. We analyse the well-posedness of the model and show existence, uniqueness and non-negativity of solutions. Moreover, we demonstrate that this model admits a non-trivial steady state, which is found to be globally stable thanks to a Lyapunov function. We finally present numerical simulations and discuss the impact of model parameters on the whole dynamics, which could constitute the main targets for pharmaceutical industry.

**Keywords** Mathematical model analysis · Steady state · Alzheimer's disease · Prions · Numerical simulations

**Mathematics Subject Classification** 34D23 · 92B05

---

This work has been supported by Association France-Alzheimer, SM 2014.

---

## 1 Introduction

### 1.1 Biological background

Alzheimer's disease (AD) is a fatal incurable disease known as the most common form of dementia [60–80% of dementia cases (Sosa-Ortiz et al. 2012)]. Affecting more than 46 million people worldwide in 2015 (Prince et al. 2015), it causes progressive neuron degeneration, leading to loss of mental functions such as memory, language or behaviour. Although AD arises most of the time in the elderly community, this disease is not considered as a normal consequence of ageing.

Causes of Alzheimer's disease remain uncertain. Different hypotheses, such as cholinergic (Francis et al. 1999), amyloid or Tau hypotheses, have been proposed to explain AD appearance. The two last hypotheses seem to be currently the most plausible ones. Indeed, accumulation of amyloid plaques inside the brain (Karran et al. 2011) and abnormalities of Tau protein are observed in diseased patients (Maccioni et al. 2010). Although these two processes could evolve simultaneously (Small and Duff 2008), it seems that the first biomarkers becoming abnormal in AD are the concentrations of amyloid  $A\beta$ -40 and  $A\beta$ -42 in patient cerebrospinal fluid (Jack et al. 2013).  $A\beta$  monomers are obtained from a specific cleavage of the amyloid precursor protein APP, leading to their release and accumulation inside the brain (Nunan and Small 2000). The major isoforms are composed of 39–43 amino acids,  $A\beta$ -40 being the most common type of monomers, and  $A\beta$ -42 a plausible evidence of Alzheimer's disease (Bitan et al. 2003; Johnson et al. 2013).  $A\beta$  monomers could at least follow two distinct polymerization pathways. The first one corresponds to the fibrillation pathway. It is well described by the canonical nucleation elongation process (Lomakin et al. 1996) with the particularity that  $A\beta$  fibrils have been reported to be able to depolymerize (Carulla et al. 2005) rendering each step of the fibrils elongation process reversible (Fig. 1, blue part). The second pathway corresponds to  $A\beta$  oligomerization. As for fibrillation, the oligomerization process follows a nucleation elongation mechanism with the difference that the oligomerization pathway leads to the formation of highly stable  $A\beta$  assemblies structurally distinct from  $A\beta$  fibrils (Nick et al. 2018; Barz et al. 2017). Regarding the literature, several neurotoxic pathways not mutually exclusive and all involving specifically  $A\beta$  oligomers have been proposed (Kessels et al. 2010; James 2013; Kandel et al. 2017). Recently one of these pathways, involving the binding of  $A\beta$  oligomers to prion protein  $PrP^C$  (its non-pathogenic monomeric conformer), has been reported to be involved in a death-signal transduction into the neurons through the oligomerization of  $PrP^C$  (Kessels et al. 2010; Gimbel et al. 2010). Even if the molecular mechanisms of this transduction signal are still unclear, the oligomerization of  $PrP^C$  (named here  $PrP^{ol}$ ) has been reported to be part of the death signal transduction (Cissé and Mucke 2009; Laurén et al. 2009; Gimbel et al. 2010). In terms of physical-chemistry, the interaction between  $PrP^C$  and  $A\beta$  oligomers leading to  $PrP^{ol}$  formation could be decomposed into two steps: the first step corresponds to the formation of  $PrP^C/A\beta$  complex (Freir et al. 2011; Gallion 2012). Then after a delay (denoted  $\tau$  in this work), corresponding to a structural rearrangement (Hilser et al. 2012), the complex evolves to generate  $PrP^C$  oligomerization.

## 1.2 Mathematical background

These processes are challenging for biologists. Indeed, it is not easy to explain the observed kinetic behaviours in experiments. Therefore an interdisciplinary collaboration between mathematicians and biologists lead to a new mathematical model where these considerations have been discussed and supported by biological assumptions and observations.

While a number of studies focus either on aggregation of  $A\beta$  monomers [see for instance Lomakin et al. (1997), Urbanc et al. (1999), Craft (2002), Achdou et al. (2013), Bertsch et al. (2016)] or on PrP<sup>C</sup> proliferation [Greer et al. (2006), Prüss et al. (2006), Engler et al. (2006), Calvez et al. (2009), Gabriel (2011), to cite a few], to the best of our knowledge, only two mathematical models have been proposed to study  $A\beta$ /PrP<sup>C</sup> interactions (Helal et al. 2014; Ciuperca et al. 2018). In the first one, authors describe plausible *in vivo* interactions between  $A\beta$  oligomers and PrP<sup>C</sup>, but did not focus on the whole process of polymerization (Helal et al. 2014). In the second article, authors propose a complex model including  $A\beta$  polymerization and interactions with prion (Ciuperca et al. 2018). However, this model assumes a continuous size for polymers, a hypothesis generally made for large number of objects, but which can be controversial for oligomers. Besides, because the model is based on partial differential equations, its analysis can be more complicated.

## 1.3 Objectives of this work

We aim herein at building a model describing *in vitro* polymerization process of  $A\beta$  monomers in fibrils or oligomers, and interactions with prion proteins, mechanisms that seem to initiate development of Alzheimer's disease. We base our model on Becker–Döring equations (Becker and Döring 1935), assuming therefore a discrete size of polymers.

Our paper is organized as follows: we first present the mathematical model proposed to describe the different mechanisms of interest. We then investigate its well-posedness and show that the model admits a unique and globally stable steady state. We finally present some numerical simulations and study the impact of model parameters on the whole dynamics.

## 2 Mathematical modelling

### 2.1 Description and notations

Our model is built in an *in vitro* context, as most experimental data are obtained *in vitro*. This means that no source or loss terms of any proteins involved in the system are considered. As a consequence, the total mass of the system should remain constant. We study evolution of  $A\beta$  monomers seeded at time  $t = 0$  in an environment containing PrP<sup>C</sup>.

The model consists of two main parts: (1) polymerization process, including formation of oligomers and fibrils and (2) interactions between oligomers and prion (Fig. 1).

During polymerization process, monomers can either form fibrils or proto-oligomers. These can then grow by attaching a monomer, or lose one at a rate  $b_f$  for fibrils and  $b$  for proto-oligomers. Rates of polymerization depend on polymer size. Indeed, we assume that longer polymers have more probability to polymerize. Proto-oligomers can reach a maximal size  $i_0$ , at which they become stable and can neither polymerize nor depolymerize. They then are called oligomers. A small proportion  $\mu$  of oligomers are still able to split into two proto-oligomers of sizes  $i$  and  $i_0 - i$ . This process is not represented in Fig. 1 for clarity.  $A\beta$  oligomers can then be transported to the amyloid plaque at a rate  $\gamma$  or form a complex with  $PrP^C$  at a rate  $\delta$ . This interaction takes an incompressible time  $\tau$  during which  $PrP^C$  is misfolded into  $PrP^{ol}$ . The oligomer is released intact from the complex and can interact with another prion or be transported to the plaque. We also add the possibility for  $PrP^C$  to directly transform into  $PrP^{ol}$  at a rate  $\alpha$ . This process can include other misfolding mechanisms that we are not aware of.

We assume that there is no fibril of infinite size, and therefore set  $i_f$  as the maximal size they can reach. Fibrils of each size are also transported in the amyloid plaque at a rate  $\gamma_f$ . As they are still able to depolymerize, monomers can escape the plaque at a rate  $b_p$ . All notations and parameters are reported in Table 1 along with their description.

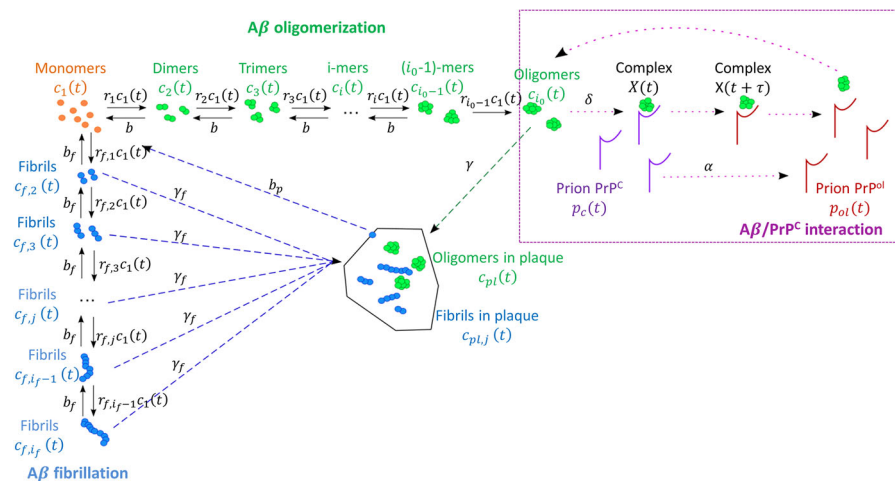


**Fig. 1** Schematic representation of  $A\beta$  polymerization processes and interactions with  $PrP^C$  prions. Orange part (top left) corresponds to monomer evolution. Blue part (left) is related to fibrillation process, while green part (top) is related to oligomerization part. Finally pink box (top right corner) corresponds to  $A\beta/PrP^C$  interaction. All parameters, quantities and interactions are described in the main text (colour figure online)

**Table 1** Description of model variables and parameters

Parameter/Variable	Definition
<i>Monomer</i>	
$c_1(t) = c_{f,1}(t)$	A $\beta$ monomer concentration
<i>Oligomerization</i>	
$i_0$	Maximal size of A $\beta$ proto-oligomers
$c_i(t), i \in \{2, \dots, i_0 - 1\}$	Size $i$ proto-oligomer concentration
$c_{i_0}(t), c_{pl}(t)$	A $\beta$ oligomer and oligomer in plaque concentrations
$r_i, i \in \{1, \dots, i_0 - 1\}$	Polymerization rate of size $i$ proto-oligomers (or monomers)
$b$	Depolymerization rate of proto-oligomers
$\gamma$	Displacement rate of A $\beta$ oligomers into the plaque
$K_{i_0,i}$	Fragmentation kernel for oligomers
$\mu$	Proportion of oligomer fragmentation
<i>Fibrillation</i>	
$i_f$	Maximal size of A $\beta$ fibrils
$c_{f,i}(t), c_{pl,i}(t), i \in \{2, \dots, i_f\}$	Size $i$ fibril and fibril in plaque concentrations
$r_{f,i}, i \in \{1, \dots, i_f - 1\}$	Polymerization rate of size $i$ fibrils (or monomers)
$b_f, b_p$	Depolymerization rates of fibrils and fibrils in plaque
$\gamma_f$	Displacement rate of A $\beta$ fibrils into the plaque
<i>A<math>\beta</math>/PrP<sup>C</sup> interaction</i>	
$p_c(t), p_{ol}(t), X(t)$	PrP <sup>C</sup> , PrP <sup>ol</sup> and A $\beta$ /PrP <sup>C</sup> complex concentrations
$\delta$	Reaction rate between A $\beta$ oligomers and PrP <sup>C</sup>
$\tau$	Duration of A $\beta$ and PrP <sup>C</sup> interaction
$\alpha$	Rate of direct transformation of PrP <sup>C</sup> into PrP <sup>ol</sup>

## 2.2 Mathematical equations

Based on Becker–Döring equations (Becker and Döring 1935), the first part of our model is as follows:

*Monomers*

$$\begin{aligned}
 c'_1(t) = & -2(r_1c_1(t)^2 - bc_2(t)) - \sum_{i=2}^{i_0-2} (r_i c_i(t)c_1(t) - bc_{i+1}(t)) - r_{i_0-1}c_{i_0-1}(t)c_1(t) \\
 & - 2(r_{f,1}c_1(t)^2 - b_f c_{f,2}(t)) - \sum_{j=2}^{i_f-1} (r_{f,j}c_{f,j}(t)c_1(t) - b_f c_{f,j+1}(t)) \\
 & + 2b_p c_{pl,2} + \sum_{j=2}^{i_f-1} b_p c_{pl,j+1}(t),
 \end{aligned} \tag{1}$$

*Proto-oligomers* ( $i \in \{2, \dots, i_0 - 2\}$ )

$$c'_i(t) = r_{i-1}c_{i-1}(t)c_1(t) + bc_{i+1}(t) - r_i c_i(t)c_1(t) - bc_i(t) + \mu K_{i_0, i} c_{i_0}(t), \quad (2)$$

$$c'_{i_0-1}(t) = r_{i_0-2}c_{i_0-2}(t)c_1(t) - r_{i_0-1}c_{i_0-1}(t)c_1(t) - bc_{i_0-1}(t), \quad (3)$$

Oligomers

$$c'_{i_0}(t) = r_{i_0-1}c_{i_0-1}(t)c_1(t) - \left(\gamma + \frac{\mu}{2}\right) c_{i_0}(t) - \delta c_{i_0}(t)p_c(t) + \delta c_{i_0}(t - \tau)p_c(t - \tau), \quad (4)$$

Oligomers in plaque

$$c'_{pl}(t) = \gamma c_{i_0}(t), \quad (5)$$

Fibrils ( $j \in \{2, \dots, i_f - 1\}$ )

$$c'_{f,j}(t) = r_{f,j-1}c_{f,j-1}(t)c_1(t) + b_f c_{f,j+1}(t) - r_{f,j}c_{f,j}(t)c_1(t) - b_f c_{f,j}(t) - \gamma_f c_{f,j}(t), \quad (6)$$

$$c'_{f,i_f}(t) = r_{f,i_f-1}c_{f,i_f-1}(t)c_1(t) - b_f c_{f,i_f}(t) - \gamma_f c_{f,i_f}(t), \quad (7)$$

Fibrils in plaque ( $j \in \{2, \dots, i_f - 1\}$ )

$$c'_{pl,j}(t) = b_p c_{pl,j+1}(t) - b_p c_{pl,j}(t) + \gamma_f c_{f,j}(t), \quad (8)$$

$$c'_{pl,i_f}(t) = -b_p c_{pl,i_f}(t) + \gamma_f c_{f,i_f}(t), \quad (9)$$

with  $t$  in  $[\tau, +\infty)$  for Eq. (4) and  $t$  in  $[0, +\infty)$  for others. For  $t$  in  $[0, \tau)$ , Eq. (4) becomes:

$$c'_{i_0}(t) = r_{i_0-1}c_{i_0-1}(t)c_1(t) - \left(\gamma + \frac{\mu}{2}\right) c_{i_0}(t) - \delta c_{i_0}(t)p_c(t). \quad (10)$$

Initial conditions are the following:

$$\begin{cases} c_1(t=0) &= m > 0, \\ c_i(t=0) &= 0, \quad i \in \{2, \dots, i_0\}, \\ c_{pl}(t=0) &= 0, \\ c_{f,j}(t=0) &= 0, \quad j \in \{2, \dots, i_f\}, \\ c_{pl,j}(t=0) &= 0, \quad j \in \{2, \dots, i_f\}, \end{cases} \quad (11)$$

which means that there are only monomers initially.

Equation (1) describes Aβ monomer evolution (orange part (top left) in Fig. 1), obtained by computing monomer gain and loss from every proto-oligomer and fibril. Equation (2) governs proto-oligomer behaviour (green part (top) in Fig. 1). Proto-oligomers of size  $i$  come from proto-oligomers of size  $i - 1$  that have attached a monomer (first term in Eq. (2)) or from proto-oligomers of size  $i + 1$  that have lost a monomer [second term in Eq. (2)]. Similarly, proto-oligomers of size  $i$  can attach or lose a monomer, and leave this compartment [third and fourth terms in Eq. (2)]. The last term in Eq. (2) describes the fragmentation process: oligomers can divide in two proto-oligomers of size lower than  $i_0 - 1$ . An extra equation is needed for proto-oligomers of size  $i_0 - 1$  [Eq. (3)] as oligomers do not depolymerize and consequently no proto-oligomers of size  $i_0 - 1$

come from an oligomer. Equation (4) describes oligomer evolution. Delayed terms express oligomer release from a complex created  $\tau$  units of time before. Finally, Eq. (5) describes the evolution of oligomers in plaque while Eqs. (6)–(7) [respectively Eqs. (8)–(9)] correspond to fibril dynamics (respectively fibrils in plaque) (blue part (left) in Fig. 1).

The second part of the model concerns  $A\beta$  oligomers and PrP<sup>C</sup> interactions (pink box (top right) in Fig. 1):

$$p'_c(t) = -\delta c_{i_0}(t)p_c(t) - \alpha p_c(t), \tag{12}$$

$$p'_{ol}(t) = \delta c_{i_0}(t - \tau)p_c(t - \tau) + \alpha p_c(t), \tag{13}$$

$$X'(t) = \delta c_{i_0}(t)p_c(t) - \delta c_{i_0}(t - \tau)p_c(t - \tau), \tag{14}$$

with  $t$  in  $[0, +\infty)$  for Eq. (12) and  $t$  in  $[\tau, +\infty)$  for Eqs. (13)–(14).

Evolution of prion concentration is given by Eq. (12): PrP<sup>C</sup> prions either form a complex with  $A\beta$  oligomer or directly transform into PrP<sup>ol</sup>. Equations (13) and (14) describe evolution of PrP<sup>ol</sup> and complexes.

On  $[0, \tau)$ , Eqs. (13)–(14) become:

$$p'_{ol}(t) = \alpha p_c(t),$$

$$X'(t) = \delta c_{i_0}(t)p_c(t),$$

and initial conditions are the following:

$$\begin{cases} p_c(t = 0) = p > 0, \\ p_{ol}(t = 0) = 0, \\ X(t = 0) = 0, \end{cases} \tag{15}$$

meaning that only PrP<sup>C</sup> are present initially.

We should now verify whether the total mass remains constant over time. We can actually divide this mass in two:  $A\beta$  polymer mass  $Q$  and prion mass  $Q_p$ :

$$Q(t) = c_1(t) + \sum_{i=2}^{i_0} i c_i(t) + \sum_{j=2}^{i_f} j(c_{f,j}(t) + c_{p,j}(t)) + i_0(c_{pl}(t) + X(t)), \tag{16}$$

$$Q_p(t) = m_p(p_c(t) + p_{ol}(t) + X(t)). \tag{17}$$

Derivatives of these functions should be equal to zero:

$$Q'(t) = \mu c_{i_0}(t) \left( \sum_{i=2}^{i_0-2} i K_{i_0,i} - \frac{i_0}{2} \right),$$

$$Q'_p(t) = 0.$$

Therefore, the fragmentation kernel should satisfy the following relation:

$$2 \sum_{i=2}^{i_0-2} i K_{i_0,i} = i_0. \tag{18}$$

This condition describes the fact that the sum of all successive fragment sizes should be equal to the initial size. Note that an oligomer can fragment either in proto-oligomers of sizes  $i$  and  $i_0 - i$  or in proto-oligomers of sizes  $i_0 - i$  and  $i$ . These two possibilities are taken into account thanks to the factor 2.

For instance, the following fragmentation kernel verifies relation (18) and guarantees mass conservation with time:

$$K_{i_0,i} = \frac{1}{i_0 - 3}, \quad i \in \{2, \dots, i_0 - 2\}.$$

This fragmentation kernel follows an uniform distribution, meaning that all fragmentations have the same probability to occur. As an example, this kernel has been used to describe the splitting of prion fibrils in Prüss et al. (2006).

### 3 Model analysis

In this section, we focus on the mathematical analysis of the model. We first present classical results of existence, uniqueness and non-negativity of solutions. We then prove the existence of a unique and non-trivial steady state. Besides, with a Lyapunov function, we show that it is globally stable, which constitutes our main result.

#### 3.1 Existence, uniqueness and non-negativity of solutions

**Proposition 1** *System of Eqs. (1)–(14) admits a unique solution on  $[0, +\infty)$ . Besides, provided that the initial conditions are non-negative, the solution remains non-negative.*

**Proof** We prove existence and uniqueness of solutions with the method of steps: we start by proving existence, uniqueness and non-negativity on  $[0, \tau)$ , then on  $[\tau, 2\tau)$ , and extend these results on intervals  $[n\tau, (n + 1)\tau)$ , for all  $n$  in  $\mathbb{N}$ .

Let us note, for all  $t$  in  $[0, +\infty)$ :

$$Z(t) = \left[ c_1(t), c_2(t), \dots, c_{i_0}(t), c_{pl}(t), c_{f,2}(t), \dots, c_{f,i_f}(t), c_{pl,2}(t), \dots, c_{pl,i_f}(t), p_c(t), p_{ol}(t), X(t) \right].$$

On  $[0, \tau)$ , the system of Eqs. (1)–(14) can be written as  $Z'(t) = H_1(t, Z(t))$ , with  $Z(0) = [m, c_2(0) = 0, \dots, c_{pl,i_f}(0) = 0, p, 0, 0]$ .  $H_1$  is a polynomial function given by:

$$H_1(Z) = \begin{pmatrix} H_{1,1}(Z) \\ r_1 Z_1^2 - bZ_2 - r_2 Z_2 Z_1 + bZ_3 + \mu K_{i_0,2} Z_{i_0} \\ \vdots \\ r_{i-1} Z_{i-1} Z_1 - bZ_i - r_i Z_i Z_1 + bZ_{i+1} + \mu K_{i_0,i} Z_{i_0} \\ \vdots \\ r_{i_0-2} Z_{i_0-2} Z_1 - bZ_{i_0-1} - r_{i_0-1} Z_{i_0-1} Z_1 \\ r_{i_0-1} Z_{i_0-1} Z_1 - (\gamma + \frac{\mu}{2}) Z_{i_0} - \delta Z_{i_0} Z_{i_0+2i_f} \\ \gamma Z_{i_0} \\ r_{f,1} Z_1^2 - b_f Z_2 - r_{f,2} Z_{i_0+2} Z_1 + b_f Z_{i_0+3} - \gamma_f Z_{i_0+2} \\ \vdots \\ r_{f,j-1} Z_{i_0+j-1} Z_1 - b_f Z_{i_0+j} - r_{f,j} Z_{i_0+j} Z_1 + b_f Z_{i_0+j+1} - \gamma_f Z_{i_0+j} \\ \vdots \\ r_{f,i_f-1} Z_{i_0+i_f-2} Z_1 - b_f Z_{i_0+i_f} - \gamma_f Z_{i_0+i_f} \\ -b_p Z_{i_0+i_f+1} + b_p Z_{i_0+i_f+2} + \gamma_f Z_{i_0+2} \\ \vdots \\ -b_p Z_{i_0+i_f+j-1} + b_p Z_{i_0+i_f+j} + \gamma_f Z_{i_0+j} \\ \vdots \\ -b_p Z_{i_0+2i_f-1} + \gamma_f Z_{i_0+1f} \\ -\delta Z_{i_0} Z_{i_0+2i_f} - \alpha Z_{i_0+2i_f} \\ \alpha Z_{i_0+2i_f} \\ \delta Z_{i_0} Z_{i_0+2i_f} \end{pmatrix},$$

where

$$\begin{aligned} H_{1,1}(Z) = & -2(r_1 Z_1^2 - cZ_2) - \sum_{i=2}^{i_0-2} (r_i Z_i Z_1 - bZ_{i+1}) - r_{i_0-1} Z_{i_0-1} Z_1 \\ & - 2(r_{f,1} Z_1^2 - b_f Z_{i_0+2}) - \sum_{j=2}^{i_f-1} (r_{f,j} Z_{i_0+j} + Z_1 - bZ_{i_0+j+1}) \\ & + 2b_p Z_{i_0+i_f+1} + \sum_{j=2}^{i_f-1} b_p Z_{i_0+i_f+j}. \end{aligned}$$

We can easily see that  $H_1$  is a locally Lipschitz continuous function with respect to  $Z$ . The Cauchy–Lipschitz theorem gives local existence and uniqueness of solutions for the system on  $[0, \tilde{\tau}]$ , for  $\tilde{\tau}$  less than or equal to  $\tau$ . The global existence of solution on  $[0, \tau)$  requires the solution to be bounded and non-negative on  $[0, \tau)$ . One can easily verifies that  $H_1$  is bounded on  $[0, \tau)$ . To prove the non-negativity of the solution,

we use the fact that an ODE system  $y' = f(y)$  on  $\mathbb{R}^n$  is called quasi-positive if the condition

$$y_i \geq 0, i \neq k \text{ and } y_k = 0 \implies f_k(y) \geq 0$$

is valid for all  $k$  in  $\{1, \dots, n\}$  (Prüss et al. 2006). In our case, the system of Eqs. (1)–(9) is quasi-positive (for  $i$  in  $\{2, \dots, i_0 - 2\}$  and  $j$  in  $\{2, \dots, i_f - 1\}$ ):

$$\begin{aligned} c_1(t) = 0 &\implies c'_1(t) = bc_2(t) + b \sum_{i=2}^{i_0-1} c_i(t) + b_f c_{f,2}(t) + b_p c_{pl,2}(t) \\ &\quad + \sum_{j=2}^{i_f} (b_f c_{f,j}(t) + b_p c_{pl,j}(t)) &&\geq 0, \\ c_i(t) = 0 &\implies c'_i(t) = r_{i-1} c_{i-1}(t) c_1(t) + b c_{i+1}(t) + \mu K_{i_0,i} c_{i_0}(t) &&\geq 0, \\ c_{i_0-1}(t) = 0 &\implies c'_{i_0-1}(t) = r_{i_0-2} c_{i_0-2}(t) c_1(t) &&\geq 0, \\ c_{i_0}(t) = 0 &\implies c'_{i_0}(t) = r_{i_0-1} c_{i_0-1}(t) c_1(t) &&\geq 0, \\ c_{pl}(t) = 0 &\implies c'_{pl}(t) = \gamma c_{i_0}(t) &&\geq 0, \\ c_{f,j}(t) = 0 &\implies c'_{f,j}(t) = r_{f,j-1} c_{f,j-1}(t) c_1(t) + b_f c_{f,j+1}(t) &&\geq 0, \\ c_{f,i_f}(t) = 0 &\implies c'_{f,i_f}(t) = r_{f,i_f-1} c_{f,i_f-1}(t) c_1(t) &&\geq 0, \\ c_{pl,j}(t) = 0 &\implies c'_{pl,j}(t) = b_p c_{pl,j+1}(t) + \gamma_f c_{f,j}(t) &&\geq 0, \\ c_{pl,i_f}(t) = 0 &\implies c'_{pl,i_f}(t) = \gamma_f c_{f,i_f}(t) &&\geq 0. \end{aligned}$$

Moreover, non-negativity of solutions of Eqs. (12)–(14) has been proven in (Ciuperca et al. 2018). Solutions on  $[0, \tilde{\tau})$  are bounded and non-negative on  $[0, \tau)$  and are therefore global solutions on  $[0, \tau)$ , and we further define  $Z(\tau) = \lim_{t \rightarrow \tau^-} Z(t)$ .

On  $[\tau, 2\tau)$ , the system of Eqs. (1)–(14) can be written as  $Z'(t) = H_2(t, Z(t), Z(t - \tau))$ , with initial conditions  $Z(\tau)$ , and where  $H_2$  is a polynomial function. Because  $Z(t - \tau)$  is known from the previous step,  $H_2$  can be written as a function of  $Z(t)$  only. Once again, it is a locally Lipschitz continuous function, bounded and non-negative on  $[\tau, 2\tau)$ . Therefore, the Cauchy–Lipschitz theorem gives existence and uniqueness of solutions on  $[\tau, 2\tau)$ .

We finally extend this result on intervals  $[n\tau, (n + 1)\tau)$ , for all  $n$  in  $\mathbb{N}$ , and prove existence, uniqueness and non-negativity of solution on  $[0, +\infty)$ .  $\square$

### 3.2 Steady state

In this section we present our main result, concerning the steady state of the model.

**Proposition 2** *System of Eqs. (1)–(14) has a unique steady state, where all variables are equal to zero, except for  $c_{pl}$  and  $p_{ol}$ :*

$$\begin{aligned} \bar{Z} &= [\bar{c}_1, \bar{c}_2, \dots, \bar{c}_{i_0}, \bar{c}_{pl}, \bar{c}_{f,2}, \dots, \bar{c}_{f,i_f}, \bar{c}_{pl,2}, \dots, \bar{c}_{pl,i_f}, \bar{p}_c, \bar{p}_{ol}, \bar{X}], \\ &= \left[ 0, 0, \dots, 0, \frac{Q}{i_0}, 0, \dots, 0, 0, \dots, 0, \frac{Q_p}{m_p}, 0, 0 \right]. \end{aligned} \tag{19}$$

Besides, this steady state is globally stable.

**Proof** We first define a reduced system, using mass Eqs. (16)–(17) and properties of Eq. (14). Indeed, we can express  $c_{pl}$  and  $p_{ol}$  as function of masses and other variables:

$$c_{pl} = \frac{1}{i_0} \left( Q - c_1(t) - \sum_{i=2}^{i_0} i c_i(t) - \sum_{j=2}^{i_f} j (c_{f,j}(t) + c_{pl,j}(t)) - i_0 X(t) \right), \tag{20}$$

$$p_{ol}(t) = \frac{Q_p}{m_p} - (p_c(t) + X(t)). \tag{21}$$

Equation (14) can be written as:

$$X(t) = \delta \int_{t-\tau}^t c_{i_0}(s) p_c(s) ds, \tag{22}$$

for  $t$  in  $[\tau, +\infty)$ . This formulation is obtained by integrating Eq. (14) on  $[\tau, +\infty)$  and by replacing  $X(\tau)$  by its value obtained when we integrate Eq. (14) on  $[0, \tau)$ .

We finally focus on the system of Eqs. (1)–(14), in which we remove equations (5), (13) and (14). This reduced system has a unique trivial steady state. Equations (20)–(22) give us the steady state for the whole system.

Steady state global stability is obtained through the following Lyapunov function:

$$\begin{aligned} V(Z) = & \sum_{i=1}^{i_0-1} i c_i(t) + \sum_{j=2}^{i_f} j (c_{f,j}(t) + c_{pl,j}(t)) + (i_0 - 1) c_{i_0}(t) + p_c(t) + X(t) \\ & + \mu \sum_{i=2}^{i_0-2} i \frac{K_{i_0,i}}{\gamma} \left( \frac{Q}{i_0} - c_{pl}(t) \right) + (i_0 - 1) \left( \frac{Q_p}{m_p} - p_{ol}(t) \right). \end{aligned} \tag{23}$$

A sketch of its construction is given below.

We define the general form of the Lyapunov function:

$$V(Z) = \sum_{j=1}^{j_N} D_j (\bar{Z}_j - Z_j) + \sum_{j=j_N+1}^N D_j Z_j,$$

where  $N$  is the number of functions,  $D_j$  are positive coefficients to determine and  $\bar{Z}$  is the steady state we study. In this form,  $Z_j$  with  $j$  in  $\{1, \dots, j_N\}$  corresponds to variables with a non-trivial steady state. In our case, these functions are thus  $c_{pl}$  and  $p_{ol}$ .

By construction, this Lyapunov function is equal to zero only at steady state and is positive elsewhere. Indeed, we can note that each variable is upper-bounded, using mass Eqs. (16)–(17). Specifically,  $c_{pl}$  is upper-bounded by  $\frac{Q}{i_0}$  and  $p_{ol}$  by  $\frac{Q_p}{m_p}$ , corresponding to the values of  $\bar{c}_{pl}$  and  $\bar{p}_{ol}$ .

We now have to choose coefficients  $D_j$  so that  $V'$  is non-positive. Let us write the  $V$  expression in our case:

$$V = \underbrace{\sum_{i=1}^{i_0-1} S_i c_i(t) + \sum_{j=1}^{i_f} M_j c_{f,j}(t) + \sum_{j=1}^{i_f} N_j c_{pl,j}(t)}_{V_1} + \underbrace{D_1 \left( \frac{Q}{i_0} - c_{pl}(t) \right) + D_2 \left( \frac{Q_p}{m_p} - p_{ol}(t) \right) + D_3 X(t) + D_4 p_c(t) + D_5 c_{i_0}(t)}_{V_2},$$

where  $S_i, i$  in  $\{1, \dots, i_0 - 1\}$ ,  $M_j, N_j, j$  in  $\{2, \dots, i_f\}$ , and  $D_k, k$  in  $\{1, \dots, 5\}$  are positive coefficients to determine, to obtain non-positive derivative of  $V$ .

Taking the  $V_1$  derivative, according to Eqs. (1)–(9) gives us:

$$V'_1 = W_1 + W_2 + W_3,$$

where  $W_1$  corresponds to the oligomerization process part,  $W_2$  to the fibrillation part and  $W_3$  to the fibrillation in plaque part.  $W_1$  can be written as follows:

$$W_1 = \sum_{i=2}^{i_0-1} S_i (G_{i-1}(t) - G_i(t) + \mu K_{i_0,i} c_{i_0}(t)) + S_{i_0-1} G_{i_0-2}(t) - S_{i_0-1} r_{i_0-1} c_{i_0-1}(t) c_1(t) - 2S_1 G_1(t) - S_1 \sum_{i=2}^{i_0-2} G_i(t) - S_1 r_{i_0-1} c_{i_0-1}(t) c_1(t),$$

where  $G_i(t) = r_i c_i(t) c_1(t) - b c_{i+1}(t)$ ,  $i \in \{1, \dots, i_0 - 2\}$  and  $G_{i_0-1}(t) = r_{i_0-1} c_{i_0-1}(t) c_1(t)$ . With these notations, we obtain:

$$W_1 = -r_{i_0-1} c_{i_0-1}(t) c_1(t) (S_{i_0-1} + S_1) + \sum_{i=2}^{i_0-1} S_i \mu K_{i_0,i} c_{i_0}(t) + \sum_{i=1}^{i_0-2} G_i(t) (S_{i+1} - S_i - S_1).$$

We take  $S_i = i S_1$ , for  $i$  in  $\{2, \dots, i_0 - 1\}$ .

$W_2$  can be written as follows (denoting  $M_1 = S_1$ ):

$$W_2 = \sum_{j=2}^{i_f-1} M_j (F_{j-1}(t) - F_j(t) - \gamma_f c_{f,j}(t)) + M_{i_f} F_{i_f-1}(t) - M_{i_f} \gamma_f c_{f,i_f}(t) - 2S_1 F_1(t) - S_1 \sum_{j=2}^{i_f-1} F_j(t),$$

where  $F_1(t) = r_{f,1}c_1(t)^2 - b_f c_{f,2}(t)$  and  $F_i(t) = r_{f,i}c_{f,i}(t)c_1(t) - b_f c_{f,i+1}(t)$ ,  $i \in \{2, \dots, i_f - 1\}$ . We then obtain:

$$W_2 = -\gamma_f \sum_{j=2}^{i_f} M_j c_{f,j}(t) + \sum_{j=1}^{i_f-1} F_j(t) (M_{j+1} - M_j - S_1).$$

In this case, we take  $M_j = jS_1$ , for  $j$  in  $\{2, \dots, i_f\}$ .

$W_3$  can be written as follows, denoting  $N_1 = S_1$  and with  $P_i(t) = -b_p c_{p,i+1}(t)$ ,  $i \in \{1, \dots, i_f - 1\}$ :

$$\begin{aligned} W_3 &= \sum_{j=2}^{i_f-1} N_j (P_{j-1}(t) - P_j(t) + \gamma_f c_{f,j}(t)) + N_{i_f} P_{i_f-1}(t) + N_{i_f} \gamma_f c_{f,i_f}(t) \\ &\quad - 2S_1 P_1(t) - S_1 \sum_{j=2}^{i_f-1} P_j(t), \\ W_3 &= \gamma_f \sum_{j=2}^{i_f} N_j c_{f,j}(t) + \sum_{j=1}^{i_f-1} P_j(t) (N_{j+1} - N_j - S_1). \end{aligned}$$

Once again, we take  $N_j = jS_1$ , for  $j$  in  $\{2, \dots, i_f\}$ .

Finally  $V'_1$  is:

$$V'_1 = -r_{i_0-1}c_{i_0-1}(t)c_1(t)(S_{i_0-1} + S_1) + \sum_{i=2}^{i_0-1} S_i \mu K_{i_0,i} c_{i_0}(t).$$

The derivative of  $V_2$  has the following expression:

$$\begin{aligned} V'_2 &= \delta c_{i_0}(t) p_c(t) (D_3 - D_4 - D_5) + \delta c_{i_0}(t - \tau) p_c(t - \tau) (D_5 - D_2 - D_3) \\ &\quad + D_5 r_{i_0-1} c_{i_0-1}(t) c_1(t) - c_{i_0}(t) \left( D_5 \left( \gamma + \frac{\mu}{2} \right) + \gamma D_1 \right) - \alpha p_c(t) (D_2 + D_4). \end{aligned}$$

We choose  $D_3 = D_4$  and  $D_2 = D_5$  to ensure negativity of the two first terms.

We finally have the following expression for  $V'$ , with the different choices made for coefficient values:

$$\begin{aligned} V' &= -r_{i_0-1}c_{i_0-1}(t)c_1(t)(i_0S_1 - D_5) + c_{i_0}(t) \\ &\quad \times \left( S_1 \mu \sum_{i=2}^{i_0-1} i K_{i_0,i} - D_5 \left( \gamma + \frac{\mu}{2} \right) - D_1 \gamma \right) \\ &\quad - D_5 \delta c_{i_0}(t) p_c(t) - D_3 \delta c_{i_0}(t - \tau) p_c(t - \tau) - \alpha p_c(t) (D_2 + D_4). \end{aligned}$$

Let us recall that this derivative should be equal to zero at steady state and negative elsewhere. To guarantee this, we finally choose  $D_5 = (i_0 - 1)S_1$  and  $D_1 = \frac{\mu \sum_{i=2}^{i_0-1} i K_{i_0,i}}{\gamma} S_1$ .

Expression (23) is finally obtained by taking  $S_1 = 1$ . By construction this function is equal to zero at steady state and positive elsewhere, with a non-positive derivative. One can easily verify that the derivative is equal to zero only at steady state.  $\square$

We prove that this model admits a unique solution, which remains non-negative provided that the initial conditions are non-negative. Moreover, we find a unique steady state, which is globally stable. From a biological point a view, this means that regardless of the initial conditions of the experiment, all monomers will eventually polymerize into oligomers that will be transported in the amyloid plaque, while all PrP<sup>C</sup> prions will be misfolded in PrP<sup>ol</sup> prions.

In the following section, we focus on the global kinetics, to comprehend the role and the impact of each parameter on the dynamics without any experimental data.

## 4 Numerical analysis

We perform a sensitivity analysis and different numerical simulations. We focus on the impact of model parameters on the dynamics of prion proteins, as they might drive the neuronal loss in Alzheimer's disease, and is the new feature in this model.

### 4.1 Numerical simulations

First, we randomly sample 5000 parameter sets and simulate the model with each of them. We arbitrarily set  $i_0 = 20$  and  $i_f = 40$ , and choose  $r_i = r_{f,i} = a \times i$  as the polymerization rate for proto-oligomers and fibrils, where  $i$  is the polymer size (number of monomers it contains). Initial values for monomers and prions are respectively  $m = 1$  and  $p = 1$ . We keep a set of parameters for which all PrP<sup>C</sup> are misconformed in PrP<sup>ol</sup>. To prevent a direct transformation of PrP<sup>C</sup> in PrP<sup>ol</sup>, we force  $\alpha$  to take a small value. Parameter values are the following, and the corresponding simulations are displayed on Fig. 2. Note that these parameters should next be estimated with experimental data, to determine optimal values and corresponding units. However, to the best of our knowledge such data are still really challenging to obtain.

$$\begin{array}{lll}
 i_0 = 20, & i_f = 40, & a = 4.7113, \\
 b = 3.0945, & b_f = 2.3194, & b_p = 3.6038, \\
 \gamma = 0.0358, & \gamma_f = 0.9675, & \delta = 3.7945, \\
 \tau = 9.4082, & \mu = 0.0168, & \alpha = 0.001.
 \end{array}$$

As expected, the mass of oligomeric prions tends to the PrP<sup>C</sup> initial value, as it is the steady state value (see Sect. 3.2). Similarly, the mass of oligomers in the plaque tends to the initial mass of A $\beta$  monomers. The misconformation of PrP<sup>C</sup> in PrP<sup>ol</sup> is mainly due to the interaction between prions and oligomers, as the value of direct transformation rate  $\alpha$  is small. Because the reaction rate between PrP<sup>C</sup> and A $\beta$  oligomers is greater than the displacement rate of oligomers into the plaque ( $\delta > \gamma$ ), oligomers are more likely to interact with prions to form complexes. After  $\tau$  units of time, they are released

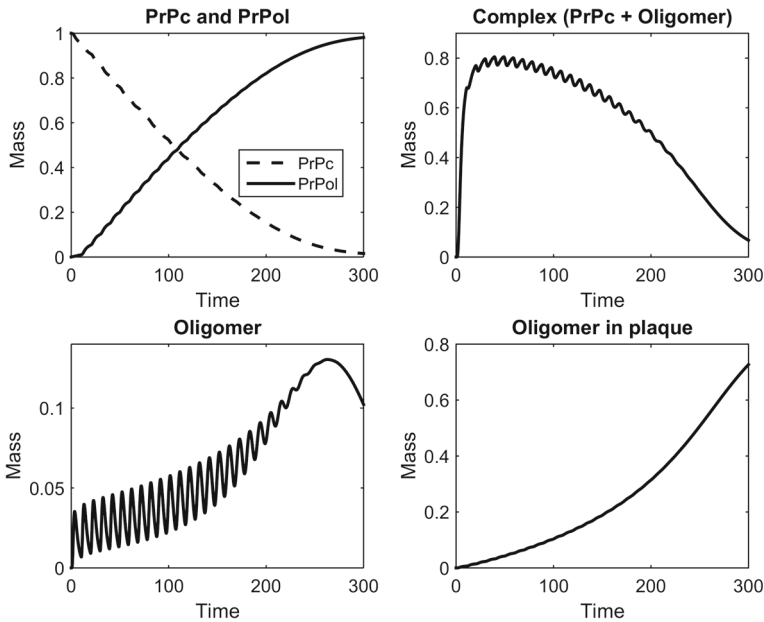


**Fig. 2** Numerical simulations with parameter values as given in the main text. Top left: Time evolution of prions  $\text{PrP}^{\text{C}}$  (dashed line) and oligomeric prions  $\text{PrP}^{\text{ol}}$  (solid line). Top right: Time evolution of  $\text{A}\beta/\text{PrP}^{\text{C}}$  complex mass (assumed to be  $i_0$ ). Bottom left: Time evolution of oligomer mass. Bottom right: Time evolution of the mass of oligomers in plaque

from this complex, causing oscillations in the evolution of complexes and oligomers. The formation of complexes decreases with time as less  $\text{PrP}^{\text{C}}$  are remaining.

#### 4.2 Sensitivity analysis

To better understand the impact of each parameter on the emergence of  $\text{PrP}^{\text{ol}}$ , we perform a sensitivity analysis through first order Sobol' indices (Iooss and Lemaître 2015) given by the following expression:

$$S_i = \frac{V(\mathbf{E}[Y|X_i])}{V(Y)}, \quad i = 1, \dots, N, \tag{24}$$

where  $Y$  is the model output (evolution of  $\text{PrP}^{\text{ol}}$  in our case),  $X_i$  is a model parameter,  $V(Y)$  represents the total variance of  $Y$ ,  $\mathbf{E}[Y|X_i]$  is the conditional mean of  $Y$  given  $X_i$ , and  $N$  is the number of model parameters. First order Sobol' indices  $S_i$  determine how much the model output varies when a parameter value varies. A parameter associated with a Sobol' index close to 1 has a large impact on  $Y$  variability, meaning that the model output is very sensitive to change in this parameter. In this work, we apply a sensitivity analysis to highlight the impact of each parameter on  $\text{PrP}^{\text{ol}}$  emergence and to determine which ones contribute most to the output. We limit our study to first order Sobol' indices. Note that the impact of the interaction of several parameters on model

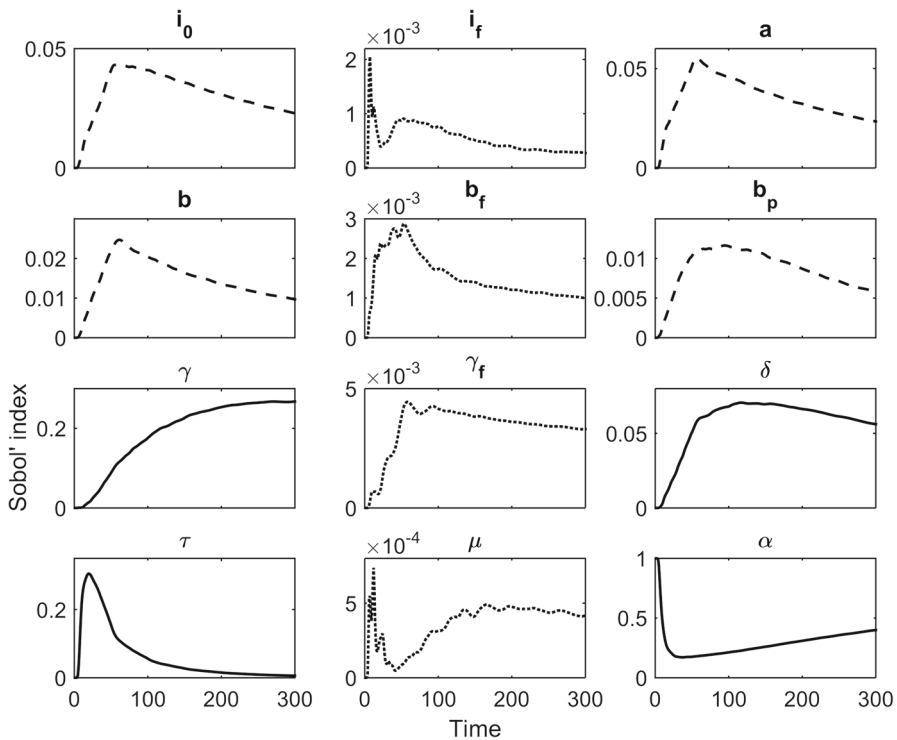


**Fig. 3** Evolution of Sobol' indices with time for each parameter. Solid lines are used for parameters impacting PrP<sup>ol</sup> emergence most, dashed lines are used for parameters with a small impact and dotted lines for parameters with no impact

output can be also be assessed through Sobol' indices, but can be more difficult to interpret. Because we do not know ranges of values for the different parameters, the interpretation of Sobol' indices should be taken with caution. Figure 3 displays results of sensitivity analysis: for each parameter, Sobol' index is calculated and its evolution with time is represented.

Based on these results, parameters can be divided in three groups:

- Parameters that impact model output most (solid lines on Fig. 3): displacement rate of oligomers in plaque  $\gamma$ , reaction rate between A $\beta$  oligomers and PrP<sup>C</sup>  $\delta$ , duration of oligomers and PrP<sup>C</sup> interaction  $\tau$  and rate of direct transformation of PrP<sup>C</sup> into PrP<sup>ol</sup>  $\alpha$ ,
- Parameters having little impact on model output (dashed lines on Fig. 3): oligomer size  $i_0$ , polymerization rate  $a$  ( $r_i = r_{f,i} = a \times i$ ) and depolymerization rates of proto-oligomers  $b$  and fibrils in plaque  $b_p$ ,
- Parameters having no impact on model output (dotted lines on Fig. 3): maximal fibril size  $i_f$ , depolymerization rate of fibrils  $b_f$ , displacement rate of fibrils in plaque  $\gamma_f$  and proportion of oligomer fragmentation  $\mu$ .

This is consistent with the role of each parameter. Indeed, we expect that parameters related to A $\beta$  oligomers/PrP<sup>C</sup> interaction play a greater role in the emergence of PrP<sup>ol</sup>.

As  $A\beta$  oligomers are required to misconform  $\text{PrP}^{\text{C}}$  in  $\text{PrP}^{\text{ol}}$ , it seems reasonable that parameters related to oligomer formation also impact  $\text{PrP}^{\text{ol}}$  emergence. However, fibrils do not interact with  $\text{PrP}^{\text{C}}$  and therefore do not impact  $\text{PrP}^{\text{ol}}$  evolution. To go further, we illustrate the impact of parameters  $a$  (polymerization rate),  $b$  (proto-oligomer depolymerization rate),  $\gamma$  (displacement rate of oligomers in plaque) and  $\delta$  (reaction rate between  $A\beta$  oligomers and  $\text{PrP}^{\text{C}}$ ). These parameters are chosen as they have a relatively strong impact on  $\text{PrP}^{\text{ol}}$  evolution. Moreover, the processes they describe could constitute new therapeutic targets to slow down the emergence of  $\text{PrP}^{\text{ol}}$ , and thus the progression of Alzheimer's disease.

### 4.3 Impact of displacement rate of oligomers into the plaque $\gamma$

Figure 4 displays the impact of parameter  $\gamma$ , the displacement rate of  $A\beta$  oligomers into plaque, on the evolution of  $\text{PrP}^{\text{ol}}$ . We perform model simulations with different values for this parameter while the others are fixed to the values given previously. We represent the evolution of  $\text{PrP}^{\text{ol}}$  (Fig. 4, top left) along with evolutions of  $A\beta/\text{PrP}^{\text{C}}$  complexes (top right),  $A\beta$  oligomers (bottom left) and oligomers in plaque (bottom right). These simulations represent the impact of  $\gamma$  on the dynamics described by the model. As expected, for small values of  $\gamma$ ,  $A\beta$  oligomers are less likely to be transported to the plaque, and therefore can bind to  $\text{PrP}^{\text{C}}$ . Consequently, more complexes are created, leading to a faster emergence of  $\text{PrP}^{\text{ol}}$ . On the contrary, for larger values of  $\gamma$ , the mass of  $A\beta$  oligomers in plaque increases faster, and therefore less  $\text{PrP}^{\text{C}}$  are misconformed in  $\text{PrP}^{\text{ol}}$ .

### 4.4 Impact of reaction rate between oligomers and $\text{PrP}^{\text{C}}$ $\delta$

Figure 5 displays the impact of  $\delta$ , the reaction rate between  $A\beta$  oligomers and prions  $\text{PrP}^{\text{C}}$  on evolutions of  $\text{PrP}^{\text{ol}}$  (top left), complexes (top right), oligomers (bottom left) and oligomers in plaque (bottom right). For small values of  $\delta$ ,  $A\beta$  oligomers are less likely to interact with  $\text{PrP}^{\text{C}}$  than to be transported in the plaque. This is the reason why we observe a stronger increase of the mass of oligomers in the plaque, while few complexes are created. For greater values of  $\delta$ ,  $A\beta$  oligomers interact with  $\text{PrP}^{\text{C}}$  and therefore more  $\text{PrP}^{\text{ol}}$  are created. We observe that for these values oligomers are found in the form of complexes or in the plaque, but few are left free.

### 4.5 Impact of polymerization rate $a$

We also study the impact of polymerization parameters on the emergence of  $\text{PrP}^{\text{ol}}$ . Although the polymerization rate  $a$  does not explicitly take part in the interaction sub-model, it impacts the evolution of  $\text{PrP}^{\text{ol}}$  through the formation of oligomers. Results of simulations for this parameter are displayed on Fig. 6. We observe that for small values of  $a$ , few  $\text{PrP}^{\text{ol}}$  are created. Indeed, because the polymerization rate is small, few oligomers are formed and therefore the interaction between  $\text{PrP}^{\text{C}}$  and  $A\beta$  oligomers is less likely to occur. As  $a$  value increases, we observe an increase in the

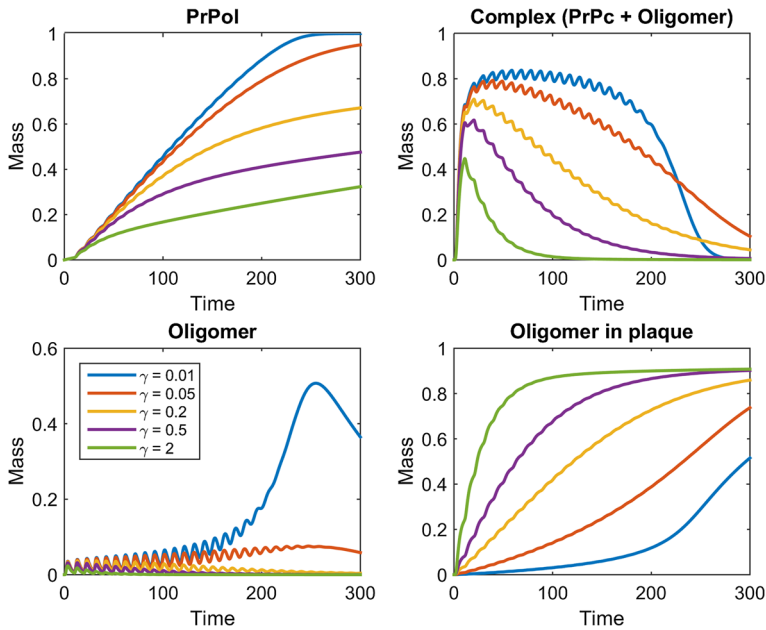


**Fig. 4** Impact of the displacement rate of oligomers into plaque  $\gamma$  on different outputs. Simulations are obtained with different values of  $\gamma$  ( $\gamma = 0.01$ : blue curve,  $\gamma = 0.05$ : red curve,  $\gamma = 0.2$ : yellow curve,  $\gamma = 0.5$ : purple curve and  $\gamma = 2$ : green curve), while other parameters are fixed to the values given previously. Top left: evolution of oligomeric prions PrP<sup>ol</sup>. Top right: evolution of A $\beta$ /PrP<sup>c</sup> complexes. Bottom left: evolution of A $\beta$  oligomers. Bottom right: evolution of A $\beta$  oligomers in plaque (colour figure online)

mass of complexes and of oligomers, leading to a faster emergence of PrP<sup>ol</sup>. We notice that the decrease of  $a$  value also slows down the increase of oligomer mass into the plaque. Indeed, as less oligomers are created, less are transported into the amyloid plaque. Consequently, the system will take more time to reach the steady state and A $\beta$  monomers remain free in the brain.

#### 4.6 Impact of depolymerization rate $b$

We finally present results of simulations for different values of the depolymerization rate of A $\beta$  proto-oligomers  $b$  (Fig. 7). For this parameter, we observe two cases. For small values of  $b$ , proto-oligomers do not depolymerize a lot, and therefore the monomer reserve cannot renew. Consequently, proto-oligomers have difficulties to evolve in bigger structures and to form oligomers. Prions PrP<sup>c</sup> are then less likely to interact with A $\beta$  oligomers and PrP<sup>ol</sup> emergence is slowed down. With greater values of  $b$ , PrP<sup>c</sup> are misconformed in PrP<sup>ol</sup> faster. Depolymerization of proto-oligomers is stronger and enables monomer concentration to remain at a sufficient level to induce polymerization process and formation of oligomers. This leads to the interaction between A $\beta$  oligomers and PrP<sup>c</sup>, and to the emergence of PrP<sup>ol</sup>. Note that for  $b = 3$ , less oligomers are present in the plaque at the end of the simulation, due to

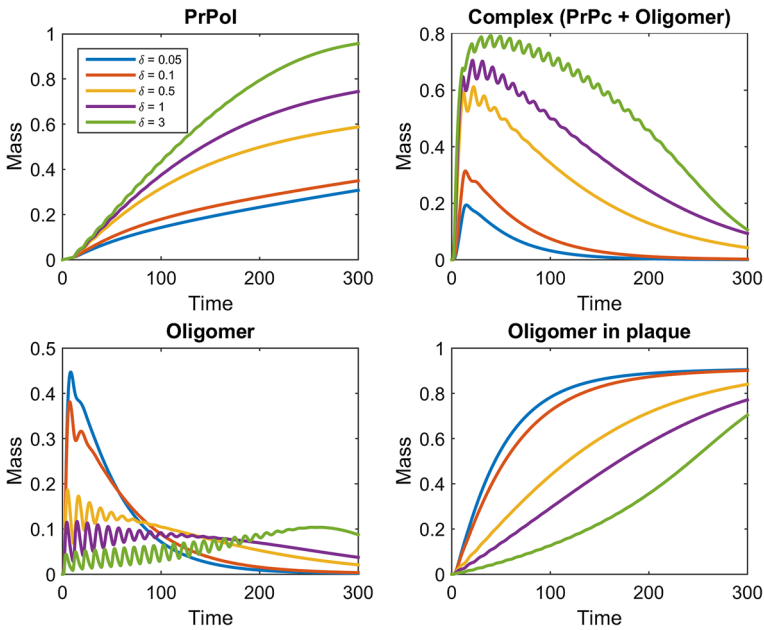


**Fig. 5** Impact of the reaction rate between  $A\beta$  oligomers and  $PrP^C$  on different outputs. Simulations are obtained with different values of  $\delta$  ( $\delta = 0.05$ : blue curve,  $\delta = 0.1$ : red curve,  $\delta = 0.5$ : yellow curve,  $\delta = 1$ : purple curve and  $\delta = 3$ : green curve), while other parameters are fixed to the values given previously. Top left: evolution of oligomeric prions  $PrP^{ol}$ . Top right: evolution of  $A\beta/PrP^C$  complexes. Bottom left: evolution of  $A\beta$  oligomers. Bottom right: evolution of  $A\beta$  oligomers in plaque (colour figure online)

polymerisation slowing down. Similarly for the effect of parameter  $a$ , we observe that for small values of  $b$ , less oligomers are transported into the amyloid plaque.

#### 4.7 Plausible therapeutic approaches?

These four parameters could constitute plausible new therapeutic targets to treat Alzheimer's disease, as they slow down the emergence of oligomeric prions, that are supposedly toxic for the neurons. However, they do not have the same impact on monomers and oligomers. Indeed, while parameters  $\gamma$  and  $\delta$  favours one mechanism between  $PrP^{ol}$  emergence and oligomer displacement into the plaque, parameters  $a$  and  $b$  also reduce the mass of oligomers in the plaque. It is then relevant to analyse monomer and proto-oligomer evolutions, to determine under which structures  $A\beta$  monomers could be found in the brain.

We perform four additional numerical simulations using parameter values as given previously. For each of these simulations, we replace  $\gamma$ ,  $\delta$ ,  $a$  or  $b$  values with the value that reduces the most the emergence of  $PrP^{ol}$  (from previous simulations), and we compare the evolution of monomers, proto-oligomers of size 10,  $PrP^{ol}$  and oligomers in the plaque (Fig. 8). As expected,  $\gamma$  and  $\delta$  have the same impact on monomer and proto-oligomer evolutions, and similar results in terms of evolutions of  $PrP^{ol}$  and oligomers in the plaque. However, because the value of  $a$  is low, few proto-

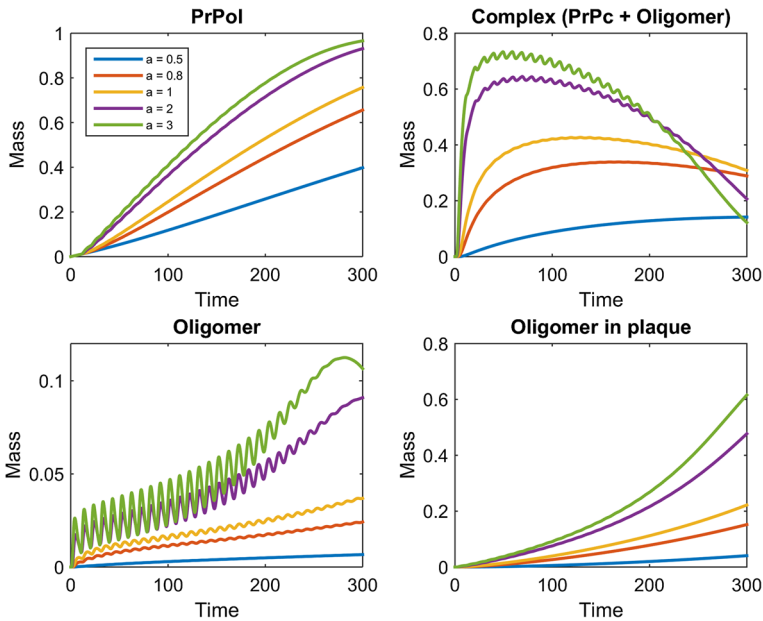


**Fig. 6** Impact of the polymerization rate  $a$  ( $r_i = r_{f,i} = a \times i$ ) on different outputs. Simulations are obtained with different values of  $a$  ( $a = 0.5$ : blue curve,  $a = 0.8$ : red curve,  $a = 1$ : yellow curve,  $a = 2$ : purple curve and  $a = 3$ : green curve), while other parameters are fixed to the values given previously. Top left: evolution of oligomeric prions  $\text{PrP}^{\text{ol}}$ . Top right: evolution of  $A\beta/\text{PrP}^{\text{C}}$  complexes. Bottom left: evolution of  $A\beta$  oligomers. Bottom right: evolution of  $A\beta$  oligomers in plaque (colour figure online)

oligomers and oligomers are created and consequently monomers remain free in the brain. The effect of  $b$  is quite the opposite: proto-oligomers are created, but because the depolymerization rate is low, the monomer reserve is not renewed and proto-oligomers cannot evolve in bigger structures and accumulate in the brain.

## 5 Discussion

$A\beta$  oligomers and prions seem to play an important role in the emergence of Alzheimer's disease although it remains to be fully understood. Recent evidence suggests that oligomers can bind to neuron membrane receptors such as prions  $\text{PrP}^{\text{C}}$ . This interaction induces first a structural re-arrangement of  $\text{PrP}^{\text{C}}$ , leading then to its oligomerization into  $\text{PrP}^{\text{ol}}$ . This last phenomenon is responsible for the transmission of a death signal to neurons and has been proposed to be one of the mechanisms responsible of neuron loss (Cissé and Mucke 2009; Laurén et al. 2009; Gimbel et al. 2010).

In this work, based on individually well characterized pathways, we present a mathematical model describing the formation of oligomers and their interaction with  $\text{PrP}^{\text{C}}$ . The sub-model for polymerization process (oligomerization and fibrillation) is composed of differential equations, based on Becker–Döring equations (Becker and

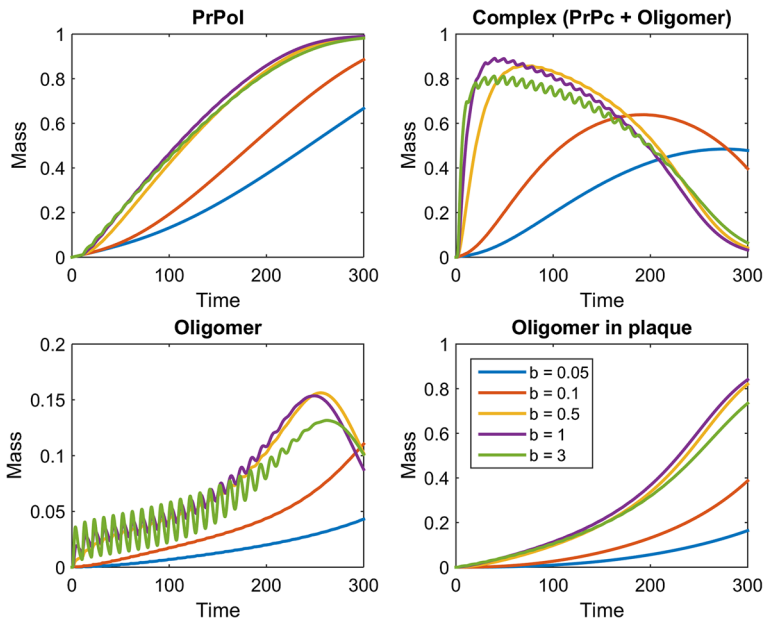


**Fig. 7** Impact of the depolymerization rate of proto-oligomers  $b$  on different outputs. Simulations are obtained with different values of  $b$  ( $b = 0.05$ : blue curve,  $b = 0.1$ : red curve,  $b = 0.5$ : yellow curve,  $b = 1$ : purple curve and  $b = 3$ : green curve), while other parameters are fixed to the values given previously. Top left: evolution of oligomeric prions  $\text{PrP}^{\text{ol}}$ . Top right: evolution of  $\text{A}\beta/\text{PrP}^{\text{C}}$  complexes. Bottom left: evolution of  $\text{A}\beta$  oligomers. Bottom right: evolution of  $\text{A}\beta$  oligomers in plaque (colour figure online)

Döring 1935). They include different mechanisms: polymerization/depolymerization, displacement in amyloid plaque and fragmentation of oligomers. The sub-model for  $\text{A}\beta/\text{PrP}^{\text{C}}$  interaction is based on delayed differential equations and describes misfolding due to this interaction as well as direct transformation of  $\text{PrP}^{\text{C}}$  into  $\text{PrP}^{\text{ol}}$ , due to possible other mechanisms we are not aware of. We prove that this model admits one unique solution, which remains non-negative for non-negative initial conditions. Moreover, the model has an unique non-trivial steady state. We demonstrate that this steady state is globally stable, through the construction of a Lyapunov function, which constitutes the main result of this work. Although the mathematical tools used in this work are quite standard, we believe that finding a relevant Lyapunov function could prove to be quite challenging. From a biological point of view, this means that, regardless of the initial conditions, the system tends to a unique state, where all monomers have polymerized in oligomers and are in the amyloid plaques, while all prions are misconformed into oligomeric prions.

We analyse the model from a numerical point of view, using sensitivity analysis and numerical simulations. We highlight the impact of different parameters, namely the reaction rate between oligomers and  $\text{PrP}^{\text{C}}$   $\delta$ , the displacement rate of oligomers in the plaque  $\gamma$ , the polymerization rate  $a$  and the depolymerization rate of proto-oligomers  $b$ , on the evolution of  $\text{PrP}^{\text{ol}}$ . We show that small values of parameters  $a$  and  $b$  slow down the emergence of oligomeric prions, as they prevent a fast polymerization into

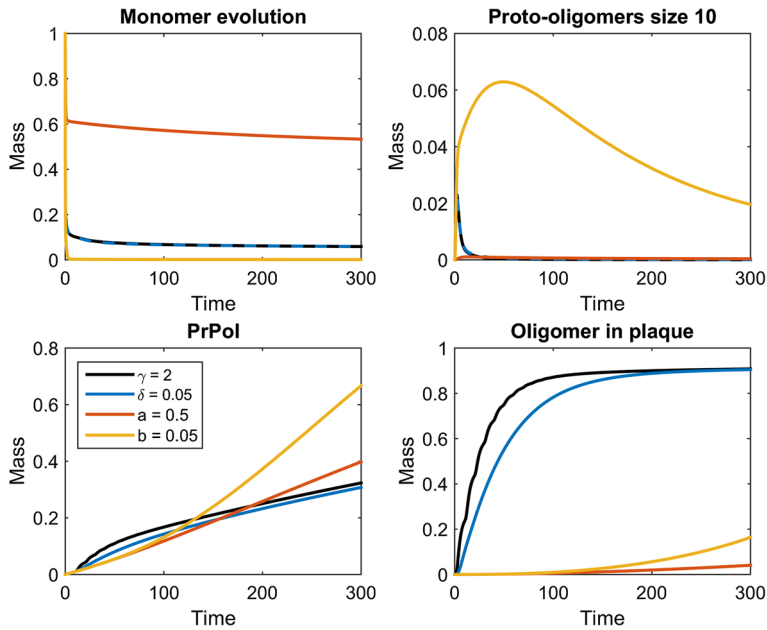


**Fig. 8** Comparison between “best” values of  $\gamma$ ,  $\delta$ ,  $a$  and  $b$  parameters, *ie* values that slow down the emergence of  $\text{PrP}^{\text{ol}}$ :  $\gamma = 2$  (black),  $\delta = 0.05$  (blue),  $a = 0.5$  (red) and  $b = 0.05$  (yellow). Top left: evolution of monomers. Top right: evolution of proto-oligomers of size 10 ( $i_0/2$ ). Bottom left: evolution of oligomeric prions  $\text{PrP}^{\text{ol}}$ . Bottom right: evolution of oligomers in the amyloid plaque (colour figure online)

oligomers. Moreover, as less oligomers are created, we see that the mass of oligomers in the amyloid plaque is drastically reduced, and therefore it will take more time for the system to reach the steady state. This is not observed for parameters  $\delta$  and  $\gamma$  because these parameters favour one mechanism between  $A\beta$  oligomers and  $\text{PrP}^{\text{C}}$  interaction and oligomer displacement into the plaque. Although our results should be assessed with experimental data, we think that these processes could constitute targets for the pharmaceutical industry, to slow down the emergence of Alzheimer’s disease (Canter et al. 2016). Different strategies could be considered. Reducing proto-oligomer polymerization or depolymerization may slow down the emergence of oligomers and therefore the emergence of oligomeric prions, but induces an accumulation of free monomers or proto-oligomers into the brain. Decreasing the reaction rate between oligomers and prions or increasing the transport of oligomers in the amyloid plaque may slow down the emergence of oligomeric prions, but oligomer mass in the plaque increases faster. One should then find the right balance between the emergence of oligomeric prions, the accumulation of monomers or proto-oligomers into the brain, and the increase of oligomers into the amyloid plaque.

To go further, experimental data is required to validate the model from a biological point of view, and estimate model parameters. Besides, the model should include two types of  $A\beta$  monomers:  $A\beta$ -40, which is the most common type of monomers present in the brain, and  $A\beta$ -42, whose presence may indicate the emergence of Alzheimer’s disease. It could be interesting to study the impact of these two types of monomers on

the whole dynamics. Indeed they do not have the same polymerization kinetics (Bitan et al. 2003; Johnson et al. 2013), and may not interact with prions in the same way, which could constitute another therapeutic strategy. However, without experimental data comparing their dynamics, it is quite difficult to model their differences.

**Acknowledgements** The authors thank Prof Glenn F. Webb for his valuable reading and corrections.

## References

- Achdou Y, Franchi B, Marcello N, Tesi MC (2013) A qualitative model for aggregation and diffusion of  $\beta$ -amyloid in Alzheimer's disease. *J Math Biol* 67(6–7):1369–92 ISSN 1432-1416
- Barz B, Liao Q, Strodel B (2017) Pathways of amyloid- $\beta$  aggregation depend on oligomer shape. *J Am Chem Soc* 140(1):319–327
- Becker R, Döring W (1935) Kinetische Behandlung der Keimbildung in übersättigten Dämpfen. *Ann Phys* 24:719–752
- Bertsch M, Franchi B, Marcello N, Tesi MC, Tosin A (2016) Alzheimer's disease: a mathematical model for onset and progression. *Math Med Biol* 34(2):193–214
- Bitan G, Kirkitadze MD, Lomakin A, Vollers SS, Benedek GB, Teplow DB (2003) Amyloid  $\beta$ -protein ( $A\beta$ ) assembly:  $A\beta$ 40 and  $A\beta$ 42 oligomerize through distinct pathways. *Proc Natl Acad Sci USA* 100(1):330–335 ISSN 0027-8424
- Calvez V, Lenuzza N, Oelz D, Deslys J-P, Laurent P, Mouthon F, Perthame B (2009) Size distribution dependence of prion aggregates infectivity. *Math Biosci* 217(1):88–99 ISSN 025-5564
- Canter RG, Penney J, Tsai L-H (2016) The road to restoring neural circuits for the treatment of Alzheimer's disease. *Nature* 539(7628):187
- Carulla N, Caddy GL, Hall DR, Zurdo J, Gairi M, Feliz M, Giralt E, Robinson CV, Dobson CM (2005) Molecular recycling within amyloid fibrils. *Nature* 436(7050):554
- Cissé M, Mücke L (2009) A prion protein connection. *Nature* 457:1090–1091 ISSN 08866236
- Ciuperca IS, Dumont M, Lakmeche A, Mazzocco P, Pujo-Menjouet L, Rezaei H, Tine LM (2018) Alzheimer's disease and prion: analysis of an in vitro mathematical model. *AIMS' Journals*. <https://hal.archives-ouvertes.fr/hal-01708659/document> (submitted)
- Craft D (2002) A mathematical model of the impact of novel treatments on the  $A\beta$  burden in the Alzheimer's brain, CSF and plasma. *Bull Math Biol* 64(5):1011–1031 ISSN 00928240
- Engler H, Prüss J, Webb GF (2006) Analysis of a model for the dynamics of prions II. *J Math Anal Appl* 324:98–117
- Francis PT, Palmer AM, Snape M, Wilcock GK (1999) The cholinergic hypothesis of Alzheimers disease: a review of progress. *J Neurol Neurosurg Psychiatry* 66(2):137–147
- Freir DB, Nicoll AJ, Klyubin I, Panico S, Mc Donald JM, Risse E, Asante EA, Farrow MA, Sessions RB, Saibil HR et al (2011) Interaction between prion protein and toxic amyloid  $\beta$  assemblies can be therapeutically targeted at multiple sites. *Nat Commun* 2:336
- Gabriel P (2011) The shape of the polymerization rate in the prion equation. *Math Comput Model* 53(7–8):1451–1456 ISSN 08957177
- Gallion SL (2012) Modeling amyloid-beta as homogeneous dodecamers and in complex with cellular prion protein. *PLoS ONE* 7(11):e49375
- Gimbel DA, Nygaard HB, Coffey EE, Gunther EC, Lauren J, Gimbel ZA, Strittmatter SM (2010) Memory impairment in transgenic Alzheimer mice requires cellular prion protein. *J Neurosci* 30(18):6367–6374 ISSN 0270-6474
- Greer ML, Pujo-Menjouet L, Webb GF (2006) A mathematical analysis of the dynamics of prion proliferation. *J Theor Biol* 242(3):598–606 ISSN 0022-5193
- Helal M, Hingant E, Pujo-Menjouet L, Webb GF (2014) Alzheimer's disease: analysis of a mathematical model incorporating the role of prions. *J Math Biol* 69(5):1207–35 ISSN 1432-1416
- Hilser VJ, Wrabl JO, Motlagh HN (2012) Structural and energetic basis of allostery. *Ann Rev Biophys* 41:585–609

- Iooss B, Lemaître P (2015) A review on global sensitivity analysis methods. In: Meloni C, Dellino G (eds) Uncertainty management in simulation-optimization of complex systems. Springer, Berlin, pp 101–122
- Jack CR Jr, Knopman DS, Jagust WJ, Petersen RC, Weiner MW, Aisen PS, Shaw LM, Vemuri P, Wiste HJ, Weigand SD et al (2013) Update on hypothetical model of Alzheimers disease biomarkers. *Lancet Neurol* 12(2):207
- James GB (2013) The role of amyloid beta in the pathogenesis of Alzheimer's disease. *J Clin Pathol* 66:362–366 ISSN 1472-4146
- Johnson RD, Schauerte JA, Chang C, Wisser KC, Althaus JC, Carruthers CJL, Sutton MA, Steel DG, Gafni A (2013) Single-molecule imaging reveals  $A\beta_{42}:A\beta_{40}$  ratio-dependent oligomer growth on neuronal processes. *Biophys J* 104(4):894–903 ISSN 00063495
- Kandel N, Zheng T, Huo Q, Tatulian SA (2017) Membrane binding and pore formation by a cytotoxic fragment of amyloid  $\beta$  peptide. *J Phys Chem B* 121(45):10293–10305
- Karran E, Mercken M, De Strooper B (2011) The amyloid cascade hypothesis for Alzheimer's disease: an appraisal for the development of therapeutics. *Nat Rev Drug Discov* 10(9):698–712 ISSN 1474-1776
- Kessels HW, Nguyen LN, Nabavi S, Malinow R (2010) The prion protein as a receptor for amyloid- $\beta$ . *Nature* 466(7308):E3
- Laurén J, Gimbel DA, Nygaard HB, Gilbert JW, Strittmatter SM (2009) Cellular prion protein mediates impairment of synaptic plasticity by amyloid- $\beta$  oligomers. *Nature* 457(7233):1128–1132 ISSN 0028-0836
- Lomakin A, Chung DS, Benedek GB, Kirschner DA, Teplow DB (1996) On the nucleation and growth of amyloid beta-protein fibrils: detection of nuclei and quantitation of rate constants. *Proc Natl Acad Sci* 93(3):1125–1129
- Lomakin A, Teplow DB, Kirschner DA, Benedek GB (1997) Kinetic theory of fibrillogenesis of amyloid beta-protein. *Proc Natl Acad Sci USA* 94:7942–7947
- Maccioni RB, Fariñas G, Morales I, Navarrete L (2010) The revitalized tau hypothesis on Alzheimer's disease. *Arch Med Res* 41(3):226–231
- Nick M, Wu Y, Schmidt NW, Prusiner SB, Stöhr J, DeGrado WF (2018) A long-lived  $A\beta$  oligomer resistant to fibrillization. *Biopolymers*. <https://doi.org/10.1002/bip.23096>
- Nunan J, Small DH (2000) Regulation of APP cleavage by alpha-, beta- and gamma-secretases. *FEBS Lett* 483(1):6–10 ISSN 00145793
- Prince M, Wimo A, Guerchet M, Ali G, Wu Y, Prina M (2015) World Alzheimer Report 2015 The Global Impact of Dementia. Alzheimer's Disease International
- Prüss J, Pujo-Menjouet L, Webb GF, Zacher R (2006) Analysis of a model for the dynamics of prions. *Discrete Contin Dyn Syst Ser B* 6(1):225–235
- Small SA, Duff K (2008) Linking  $A\beta$  and tau in late-onset Alzheimer's disease: a dual pathway hypothesis. *Neuron* 60(4):534–542
- Sosa-Ortiz AL, Acosta-Castillo I, Prince MJ (2012) Epidemiology of dementias and Alzheimer's disease. *Arch Med Res* 43(8):600–608 ISSN 01884409
- Urbanc B, Cruz L, Buldyrev SV, Havlin S, Irizarry MC, Stanley HE, Hyman BT (1999) Dynamics of plaque formatio in Alzheimer's disease. *Biophys J* 76:1330–1334 ISSN 0006-3495

## Affiliations

Mohammed Helal<sup>1</sup> · Angélique Igel-Egalon<sup>2</sup> · Abdelkader Lakmeche<sup>1</sup> ·  
 Pauline Mazzocco<sup>3</sup> · Angélique Perrillat-Mercerot<sup>4</sup> ·  
 Laurent Pujo-Menjouet<sup>5,6</sup> · Human Rezaei<sup>2</sup> · Léon M. Tine<sup>5,6</sup>

✉ Laurent Pujo-Menjouet  
 pujo@math.univ-lyon1.fr

<sup>1</sup> Laboratory of Biomathematics, University Sidi Bel Abbes, Sidi Bel Abbès, Algeria

<sup>2</sup> UR892 Virologie Immunologie Moléculaires, INRA, 78352 Jouy-en-Josas, France

- <sup>3</sup> CNRS UMR 5558, Laboratoire de Biométrie et Biologie Evolutive, Université Claude Bernard Lyon 1, Université de Lyon, 69100 Villeurbanne, France
- <sup>4</sup> Laboratoire de Mathématiques et Applications, UMR CNRS 7348, SP2MI Equipe DACTIM-MIS, Université de Poitiers, 86962 Chasseneuil Futuroscope Cedex, France
- <sup>5</sup> CNRS UMR 5208 Institut Camille Jordan, Université Claude Bernard Lyon 1, Université de Lyon, 69622 Villeurbanne Cedex, France
- <sup>6</sup> Inria Team Dracula, Inria Grenoble Rhône-Alpes Center, 69100 Villeurbanne, France